



HAL
open science

A complete FE simulation tools for NDT inspections with piezoelectric transducers

Sebastien Imperiale, Simon Marmorat, Nicolas Leymarie, Sylvain Chatillon

► **To cite this version:**

Sebastien Imperiale, Simon Marmorat, Nicolas Leymarie, Sylvain Chatillon. A complete FE simulation tools for NDT inspections with piezoelectric transducers. Acoustics 2012, Apr 2012, Nantes, France. hal-00811151

HAL Id: hal-00811151

<https://hal.science/hal-00811151>

Submitted on 23 Apr 2012

HAL is a multi-disciplinary open access archive for the deposit and dissemination of scientific research documents, whether they are published or not. The documents may come from teaching and research institutions in France or abroad, or from public or private research centers.

L'archive ouverte pluridisciplinaire **HAL**, est destinée au dépôt et à la diffusion de documents scientifiques de niveau recherche, publiés ou non, émanant des établissements d'enseignement et de recherche français ou étrangers, des laboratoires publics ou privés.



ACOUSTICS 2012

A complete FE simulation tools for NDT inspections with piezoelectric transducers

S. Imperiale^{a,b}, S. Marmorat^{a,b}, N. Leymarie^a and S. Chatillon^a

^aCEA LIST, Centre de Saclay - point courrier 120, 91191 Gif-Sur-Yvette, France

^bPOEMS, INRIA Rocquencourt, 78153 Le Chesnay, France

sebastien.imperiale@inria.fr

An ultrasonic inspection system involves the generation, propagation and reception of short transient signals. Piezoelectric transducers and particularly phased arrays are increasingly used in ultrasonic Non Destructive Testing (NDT) because of their ability to focus or deflect an ultrasonic beam in parts of complex geometries. To accurately model the sensitivity in transmission and reception of such sensors, a transient Finite Element (FE) model has been developed including not only piezoelectric effects but also complex electrical impedance conditions modeling the effect of elements of a pulser/receiver system. A particular attention is devoted to these electrical and mechanical boundary conditions used to model the emission and reception regimes of the sensor. The definition of the inspection domain is made easier by a decomposition domain technique allowing, in the same time, local time stepping and efficient absorbing layers to optimize calculation cost. In order to illustrate all the capabilities of this simulation tool, several cases of NDT inspections are then presented through the analysis of the ultrasonic beam snapshots and the electrical signal read on the receiver.

1 Introduction

Because of their ability to focus or deflect an ultrasound beam in complex shaped components, phased arrays are increasingly used in ultrasonic nondestructive testing. These probes are usually made of piezo-composite materials reducing the cross-coupling between adjoining elements. In order to model accurately the sensitivity in transmission and reception of such sensors, a transient Finite Element model has been developed. The objective of this work initiated between the CEA LIST and the POEMS project aims to accurately model the response of electro-acoustic piezoelectric sensors by a finite element (FE) method. Numerous studies by FE methods deal with this vast subject [1, 2, 3, 4]. The proposed FE code has taken benefits from the techniques developed by the project teams POEMS. It is particularly based on a transient FE method dealing with mixed spectral FE and taking into account piezoelectric effects. Decomposition domain techniques are also used to facilitate the meshing of individual objects which are included in an ultrasonic testing scene (piece, piezoelectric element, matching layer, backing, coupling media ...). This decomposition technique allows to optimize the numerical schemes in each domain (local time step technique, differentiated management fluid domain or solid domain). Initially, a description of the problem is made detailing all the modelling domains taken into account: sensor, wedge, sample. In a second part, we describe the mathematical formulation of the problem and its discretization. Then the different optimization techniques used are detailed. Finally, some simulations are proceeded to illustrate all the capabilities of this code.

2 Mathematical model

2.1 General description of the problem

For the modelling of an inspection configuration, the main object of interest is the transducer (cf. Figure 1). The ultrasonic sensor is considered to be composed by a piezoelectric block. On its upper side, a backing layer is usually used to dissipate the acoustic energy going out the back of the transducer. On the other side, a matching layer can be used to efficiently propagate the wave into the coupling medium. This layer is often a quarter wavelength thick and made of a material which has an acoustic impedance midway between that of the piezoelectric material and the coupling medium. According to the case of application considered, the coupling medium may be a fluid (water), a wedge of polymer (Plexiglass) or the sensor may be directly in contact with the part.

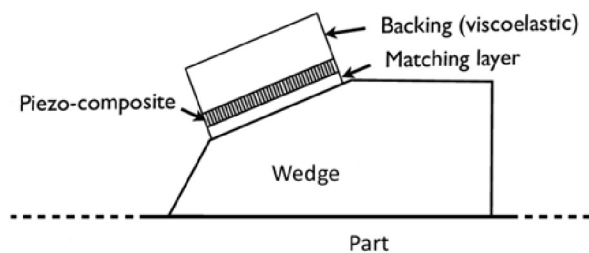


Figure 1: Description of the various components considered for the simulation of an ultrasonic testing.

In the most general case, the piezoelectric block, represented by the domain Ω_p , may be a heterogeneous medium such as piezo-composite materials composed of distributed piezoceramic bars embedded in a polymer matrix. This block is connected to several electrodes localized on the top and a unique mass electrode on the bottom (cf. Figure 2).

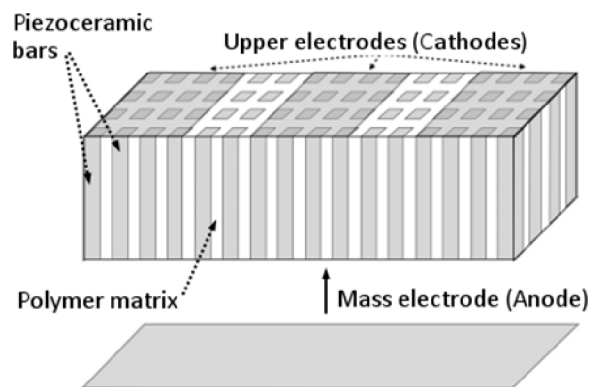


Figure 2: Schematic illustration of the piezo-composite block with the positioning of electrodes.

For simplicity, these electrodes, which are in practice very thin, will be considered as connected surfaces.

2.2 Mathematical formulation and discretization

2.2.1 Piezoelectric equation and boundary conditions

The equation of piezoelectricity results from the coupling of the Maxwell's and elastodynamic equations. Using the classical quasi-static approximation we reduce the electric unknowns to a scalar electric potential. Considering the large contrast of permittivity in the piezocomposite between rods and the embedding polymer, we have justified the reduction of the computation to the piezoelectric domains only [1].

Then, in a piezoelectric domain Ω_P , the full system to be solved couples the classical elastodynamic equation for displacement u with a Laplace equation for the electrical potential φ , such as:

$$\begin{cases} \rho \partial_{tt} u - \text{div}(\mathbf{C}\varepsilon(u) - \mathbf{d}\nabla\varphi) & = 0 \\ \text{div}(\varepsilon\nabla\varphi - \mathbf{d}^T \varepsilon(u)) & = 0 \end{cases} \quad (1)$$

with $\varepsilon(u) = \frac{1}{2}(\partial_i u_j + \partial_j u_i)$. ρ is the density, \mathbf{C} the elastic tensor and \mathbf{d} is the piezoelectric tensor coupling both electrical and mechanical components.

The electrical potential is assumed to be constant in space along each electrode which means electrodes are considered as perfect conductors. The emission and reception processes are defined through well-chosen boundary conditions. The i^{th} anode, denoted with Γ_i^a boundary, is connected to a common mass, which imposes a reference potential such as $\varphi|_{\Gamma_i^a} = 0$ for instance. For the cathode, we use a simplified model (see [5] for more sophisticated ones or [6] for similar approaches). The electric charge on the i^{th} cathode is defined by

$$Q_i(t) = \int_{\Gamma_i^c} (\varepsilon\nabla\varphi - \mathbf{d}^T \varepsilon(u)) \cdot \mathbf{n} \, d\sigma. \quad (2)$$

Each cathode is considered independently of the others. During the emission process, a short transient excitation is applied from a generator on the i^{th} cathode imposing an electrical potential denoted V_i . This source term is coupled with a relationship on the electrode based on Ohm's law in the case of a quasi-static approximation. Finally, assuming that each piezoceramic bar is decoupled with the other with $I_i = dQ_i/dt$, then we obtain the mixed boundary condition:

$$\varphi|_{\Gamma_i^c} = V_i + R_i \frac{d}{dt} \int_{\Gamma_i^c} (\varepsilon\nabla\varphi - \mathbf{d}^T \varepsilon(u)) \cdot \mathbf{n} \, d\sigma, \quad (3)$$

on the part Γ_i^c of the bar in contact with the cathode of the i^{th} element where R_i is the electrical impedance of the generator. More details about all the boundary conditions to close the problem are given in a paper recently published [7].

Finally, in order to bound the computational domain, we have developed an efficient technique based on the approach to design perfectly matched layers (PML) for transient wave equations. Our approach is based, first, on the introduction of a modified wave equation and, second, on the formulation of general "perfectly matched" transmission conditions for this equation. The validity of our approach in terms of stability and accuracy is discussed in [8]. This technique using constant damping coefficients and combined with high order elements is very efficient and allows one to reduce the size of PML when we want to impose absorbing condition.

2.2.2 Discretization

The implemented numerical method handles the problem by combining high order Galerkin finite elements and explicit time discretization [9]. High order spectral finite element methods were chosen because of their excellent performance while having a low memory and computational cost. The discretization is performed using an intern approximation of the space $H^1(\Omega_P)$. The approximation space is defined from $\widehat{K} = [0, 1]^d$ the reference square or cube, where d denotes the dimension of the problem. We use a mesh \mathcal{M}_h of Ω_P , composed of quadrangles in 2D and hexahedrons in

3D denoted K_j . Set $\mathbf{F}_j = (F_{j,1} \dots F_{j,d})$ the mapping such that $\mathbf{F}_j(\widehat{K}) = K_j$. On this mesh, we can define the subspace of $H^1(\Omega_P)$

$$U_h^r(\Omega_P) = \{v_h \in H^1(\Omega_P) \text{ such that } v_h|_{K_j} \circ \mathbf{F}_j \in \mathcal{Q}_r\}, \quad (4)$$

where \mathcal{Q}_r is the polynomial space spanned by the polynomials of order less than $d \times r$. The use of elements defined on \widehat{K} enables to define the basis function $\hat{\varphi}$ as a tensor product of 1D functions, in the following way

$$\hat{\varphi}_j(\mathbf{x}) = \prod_{k=1}^d \hat{\varphi}_{j_k}(x_k). \quad (5)$$

Letting $\{\hat{\xi}_p\}$, $p = 1..r+1$, denotes the set of Gauss-Lobatto quadrature points (see [9]). We define the polynomials $\hat{\varphi}_{j_k}$ of order r from the following relation

$$\hat{\varphi}_{j_k}(\hat{\xi}_p) = \delta_{jkp} \quad \forall p = 1..r+1, \quad (6)$$

where δ_{jkp} is the Kronecker delta.

We look for $u_h \in [U_h^r(\Omega_P)]^d$ and $\varphi_h \in U_h^r(\Omega_P)$. We decompose these two unknowns on the lagrangian basis functions, write down the variational formulation arising from (1) and test the equality against all the basis functions. We compute the integrals at stake using Gauss-Lobatto quadrature rule, which is exact for polynomials of order less than $2r-1$ and consistent at order r . We obtain the following system (see [7] for more details and the treatment of the boundary conditions at a discrete level)

$$\begin{aligned} \mathcal{M} \frac{d^2}{dt^2} u_h + \mathcal{K} u_h + \mathcal{B}^T \varphi_h &= -\mathcal{B}^T V_h, \\ C \varphi_h &= \mathcal{B} u_h. \end{aligned} \quad (7)$$

We can eliminate the unknown φ_h to obtain

$$\mathcal{M} \frac{d^2}{dt^2} u_h + (\mathcal{K} + \mathcal{B}^T C^{-1} \mathcal{B}) u_h = -\mathcal{B}^T V_h. \quad (8)$$

The choice of basis functions and quadrature points ensures essential properties to the matrices at stake in (8). The matrix \mathcal{M} is diagonal and positive-definite. The matrices \mathcal{B} , C and \mathcal{K} are symmetrical, positive-semidefinite and can be factorized to perform a reduction of the computational and memory cost of the algorithm (as explained in [9]).

It only remains to complete a time discretization of (8). As explained in [7], second orders finite difference scheme are used. The stability of the fully discrete numerical schemes is then guaranteed over an explicit time step restriction.

2.2.3 Domain decomposition and local time step

To handle the discretization of complex shaped objects or high heterogeneous media, a domain decomposition methods using Mortar elements has been implemented (see [10] for instance). It enables to mesh these domains independently (see side-drilled hole in figure 3) of the mesh used for the surrounding medium or for the piezoelectric sensors. It is also useful when one wants to deal with a configuration in which different physical phenomenons are implied (for instance fluid-structure interaction).

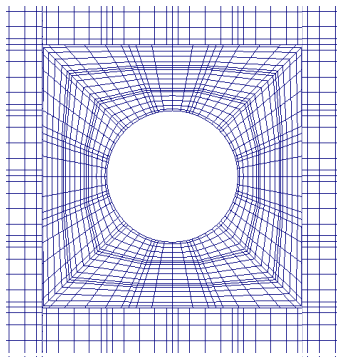


Figure 3: Circular hole meshing in a homogenous medium. Every intersection corresponds to the localization of a high order nodal FE basis function. The domain decomposition method enables to deal with non-conforming interfaces

For the sake of simplicity, we briefly present the domain decomposition method for acoustic waves. Consider two domains Ω_1 and Ω_2 with a common frontier $\Gamma = \partial\Omega_1 \cap \partial\Omega_2 \neq \emptyset$, and set $\Omega = \Omega_1 \cup \Omega_2$. We wish to compute u the solution of

$$\partial_{tt}u - \Delta u = f, \quad x \in \Omega, \quad t > 0,$$

where f is a source term with support contained into Ω_1 .

It is well-known that this is equivalent to looking for the solutions u_1, u_2 of

$$\begin{cases} \partial_{tt}u_1 - \Delta u_1 = f, & x \in \Omega_1, \quad t > 0, \\ \partial_{tt}u_2 - \Delta u_2 = 0, & x \in \Omega_2, \quad t > 0, \end{cases}$$

with the matching conditions on the interface

$$u_1 = u_2, \quad \nabla u_1 \cdot \mathbf{n} = \nabla u_2 \cdot \mathbf{n}, \quad \mathbf{x} \in \Gamma, \quad t > 0.$$

Then, the mortar element method consists in introducing the Lagrange multiplier λ such that

$$\partial_t \lambda = \nabla u_1 \cdot \mathbf{n} = \nabla u_2 \cdot \mathbf{n},$$

and to look for the traces continuity under a weak form:

$$\langle u_1, \mu \rangle_{\frac{1}{2}, -\frac{1}{2}} = \langle u_2, \mu \rangle_{\frac{1}{2}, -\frac{1}{2}}, \quad \forall \mu \in H^{-1/2}(\Gamma), \quad t > 0.$$

One can now derive an adapted formulation for the implementation of the finite element method on the different subdomains Ω_1 and Ω_2 , while computing a finite element space on the interface Γ to compute the Lagrange multiplier λ .

This method enables us to compute the solution in each subdomain "independently", modulo the computation of the Lagrange multiplier λ on the interface. However the time step of the global simulation is still affected by any small element used around the defects. Another example is a strong speed contrast between two mediums, which is typically the case when one wants to deal with fluide-structure problems. To circumvent this difficulty the energy preserving local time step procedure developed in ([11],[12]) is used. This local time step technique enables to choose different time step in each domain of the global simulation domain. Through energy preservation, the stability of the schemes is guaranteed over explicit time step restrictions.

3 Numerical results

Angular beam deflection with linear array probe

As a first example, we have performed two 2D simulations in order to calculate the radiated beam from a phased

array wedge probe: one with a uniform delay law, the other with a linear delay law. The figure 4 presents a comparison of the radiated beam for several time steps of the calculation process. As expected, the linear delay law imposed on each

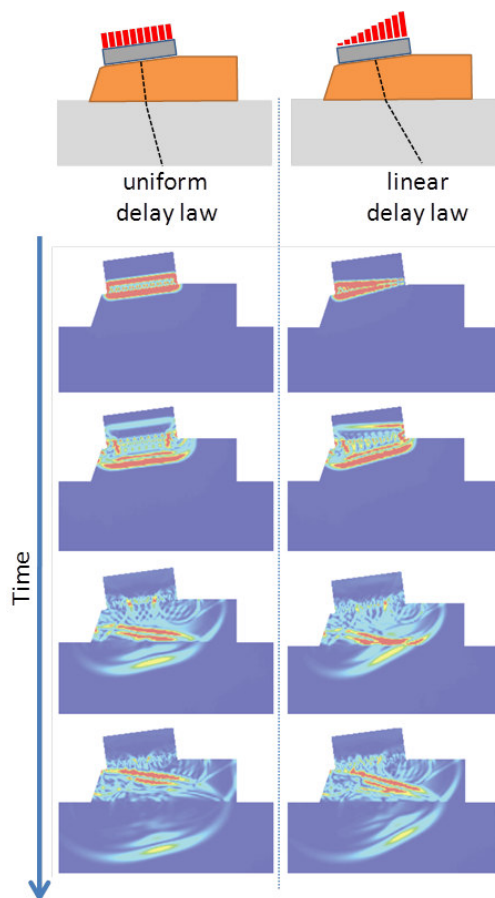


Figure 4: Description of the various components considered for the simulation of an ultrasonic testing.

element induces a deflection of the radiated beam. The multiple reflections in the wedge can be fully simulated as well as the transmitted beam in the sample. These informations appear to be of great interest in the design of ultrasonic sensors.

Beam focusing with linear array probe on a side-drilled hole

This time, we present another 2D configuration to illustrate the effect of an electronic focusing on the response of a typical defect such as a side-drilled hole. We consider a phased array probe directly in contact with an isotropic homogeneous half-space in which a side-drilled hole is embedded (see figure 5). We use stress free condition on all the elastic boundaries and perfectly matched layer are used to bound the computational domain. As a reference, we first consider the case of a uniform delay law. In the second simulation, the delay law applied on each cathode is defined to focus the radiated beam energy at the depth of the considering defect. In the figure 6, we present the comparison of the radiated beam for the two different cases at several time steps. As expected, in the case of the focused beam, the energy of the reflected wave is higher than the one performs with a uniform

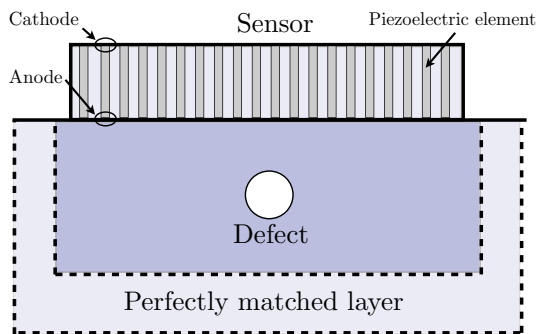


Figure 5: Schematic view of the testing configuration.

law. As a consequence, if we observe the electronic signal

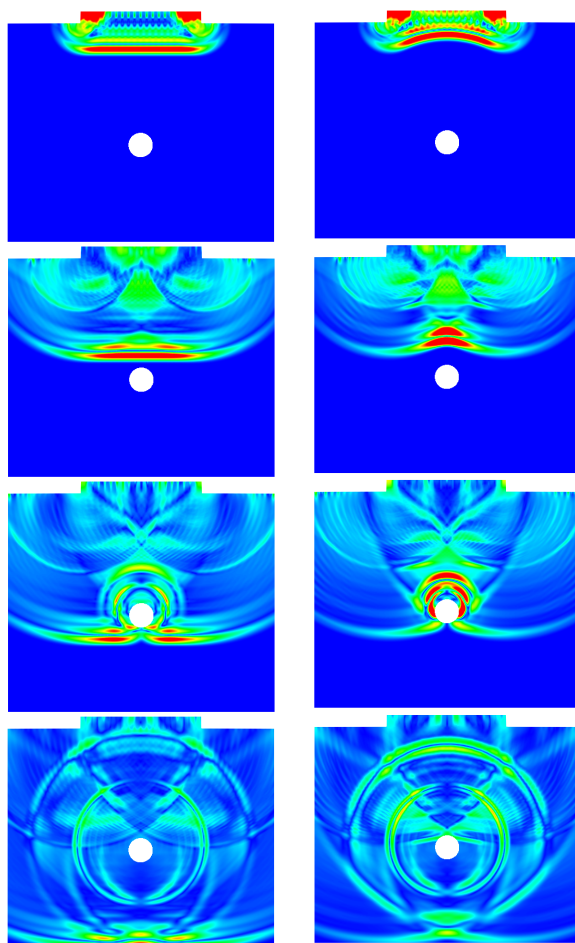


Figure 6: Snapshots of the absolute value of the displacement at $t = 0.52, 1.04, 1.57, 4.71, 5.24, 5.76, 6.81, 8.39, 9.96$. The electrodes are excited without delay (left figures) and with delay (right figures).

read on one electrode placed at the middle of the sensor, the maximum amplitude is twice as large in the "focusing" case in comparison with the "uniform" case.

4 Conclusion

We have developed a finite element code to simulate an ultrasonic inspection as a whole involving the generation, propagation and reception of short transient signals. Phased array transducers can be model in transmission and reception including not only piezoelectric effects but also complex

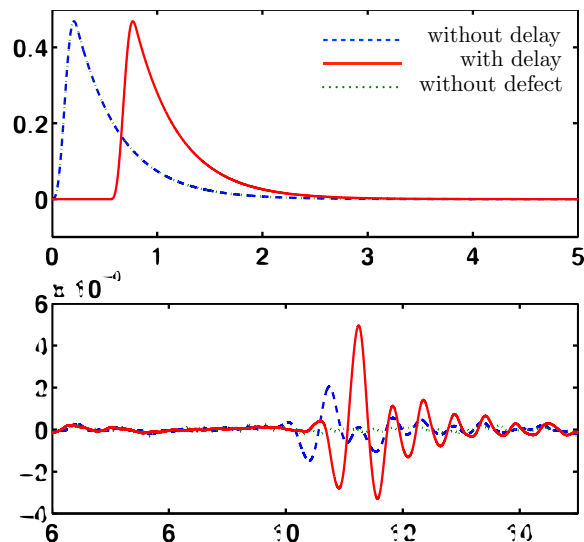


Figure 7: Value of the potential versus time recovered on the electrode placed at the middle of the sensor.

electrical impedance conditions to model the pulser/receiver system. Different techniques are used to optimize calculation cost and limit the cost of memory storage: high order element, decomposition domain, local time stepping and efficient absorbing layers. The capabilities of this simulation tool has been shown in several cases of NDT inspections. However this code has not yet been validated against analytical models (1D) and experimental measurements. These will be the subject of our future studies.

References

- [1] A. C. Hladky-Hennion, J. N. Decarpigny, "Finite element modeling of active periodic structures: application to 1-3 piezocomposites", *J. Acoust. Soc. Am.* **94** (1), 621-635 (1993)
- [2] R. Lerch, "Simulation of Piezoelectric Devices by Two- and Three-Dimensional Finite Elements", *IEEE Transactions on Ultrasonics, Ferroelectrics and Frequency Control* **37** (2), 233-247 (1990)
- [3] Y. Ricon, F. Montero de Espinosa, "Piezoelectric modelling using a time domain finite element program", *Journal of the European Ceramic Society* **27** (13-15), 4153-4157 (2007)
- [4] M. Kaltenbacher, R. Lerch, "Perfectly Matched Layer Technique for the Numerical Computation of Wave Propagation Phenomena", *IEEE Ultrasonics Symposium* (2007)
- [5] L. Schmerr Jr. and S. J. Song, "Ultrasonic Nondestructive Evaluation Systems", *Springer*, New York
- [6] E. Canon, M. Lenczner, "Models of elastic plates with piezoelectric inclusions part I: Models without homogenization", *Mathematical and Computer Modelling* **5** (26), 79-106 (1997)
- [7] S. Impériale, P. Joly, "Mathematical and numerical modelling of piezoelectric sensors", *Mathematical Modelling and Numerical Analysis* **46** (4), 875-909 (2012)

- [8] E. Demaldent, S. Impériale, "Perfectly matched transmission problem with absorbing layers: application to anisotropic acoustics", *Int. J. Numer. Meth. Engng*, submitted (2012)
- [9] G. Cohen, "High order numerical methods for transient wave equation", *Springer*, Berlin (2001)
- [10] A. Bendali, Y. Boubendir, "Non-overlapping domain decomposition method for a nodal finite element method", *Numerische Mathematik***103** (4), 515-537 (2006)
- [11] F. Collino, T. Fouquet, P. Joly, "A conservative space-time mesh refinement method for the 1-d wave equation. Part I: Construction", *Numerische Mathematik***95** (2), 197-221 (2003)
- [12] E. Bécache, P. Joly, J. Rodríguez, "Space-time mesh refinement for elastodynamics. Numerical results", *Computer Methods in Applied Mechanics and Engineering***194** (2-5), 355-366 (2005)